Crystallization of amorphous silicon beyond the crystallized polycrystalline silicon region induced by metal nickel*

Dongli Zhang(张冬利)[1,2], Mingxiang Wang(王明湘)[1,†], Man Wong(王文)[2], and Hoi-Sing Kwok(郭海成)[2]

[1] *Department of Microelectronics, Soochow University, Suzhou* 215006, *China*

[2] *Center for Display Research, Department of Electronic and Computer Engineering, the Hong Kong University of Science and Technology, Kowloon, Hong Kong, China*

(Received 29 August 2016; revised manuscript received 25 October 2016; published online 30 November 2016)

Crystallization of amorphous silicon (a-Si) which starts from the middle of the a-Si region separating two adjacent metal-induced crystallization (MIC) polycrystalline silicon (poly-Si) regions is observed. The crystallization is found to be related to the distance between the neighboring nickel-introducing MIC windows. Trace nickel that diffuses from the MIC window into the a-Si matrix during the MIC heat-treatment is experimentally discovered, which is responsible for the crystallization of the a-Si beyond the MIC front. A minimum diffusion coefficient of 1.84×10^{-9} cm^2/s at 550 °C is estimated for the trace nickel diffusion in a-Si.

Keywords: metal-induced crystallization, poly-Si, nickel, diffusion coefficient

PACS: 66.30.Dn, 81.05.Gc, 68.35.bg **DOI:** 10.1088/1674-1056/26/1/016601

1. Introduction

Low-temperature polycrystalline silicon (poly-Si) technology has been intensively studied for various kinds of applications, such as active-matrix flat-panel displays, three-dimensional integrated circuits, and thin-film solar cells. Metal-induced crystallization (MIC) of amorphous silicon (a-Si) is one of the low-temperature fabrication technologies that can achieve high quality poly-Si. Choices for the crystallization metallic catalysts include nickel (Ni),[1] aluminum,[2,3] copper (Cu),[4] palladium (Pd),[5] etc., among which Ni-based MIC has been most widely investigated.

Though there have been many variations of Ni-based MIC technology, such as confining crystallization catalyst nickel to specified regions for longitudinal poly-Si grains[6–8] or introducing tiny amount of nickel uniformly or randomly for large domain poly-Si,[9–12] the same crystallization mechanism is involved, i.e., the formation and migration of Ni silicide at the crystallization front.[13–15] When there is sufficient nickel at the crystallization front, a large amount of crystallization nuclei will be formed and poly-Si grains can grow simultaneously at the same speed such that the interface between the MIC poly-Si and the uncrystallized a-Si can keep smooth, but it will become ragged if the amount of nickel at the crystallization front is insufficient.[16]

For Cu- and Pd-based MIC, it has been reported that the lateral crystallization rates could be enhanced by reducing the separation between adjacent crystallization-inducing metal regions. For Cu, such a proximity effect is attributed to heat generation and accumulation[4] and for Pd, it is explained with the diffusion of Pd in a-Si.[5] For Ni-based MIC, dependences of the crystallization rate on the a-Si island length and the presence of a metal-gettering region have also been reported.[14] In this paper, we report the observation of the crystallization of the a-Si from the middle of the a-Si region that separates two neighboring MIC poly-Si regions. Trace Ni diffuses from the MIC windows and accumulates in the a-Si beyond the MIC poly-Si is experimentally discovered and such trace Ni induced crystallization is responsible for the observed crystallization phenomenon.

2. Experiments

The 4-inch silicon wafers covered with 500-nm thermal oxide were used as the starting substrates. Two kinks of crystallization samples were prepared. By using plasma-enhanced chemical vapor deposition (PECVD) at a substrate temperature of 200 °C, 500-nm a-Si:H was deposited on Type-I samples and 50-nm a-Si:H was deposited on Type-II samples. Before the deposition of 300-nm PECVD SiO_2 and subsequent MIC windows definition, phosphorus implantation at a dosage of 1×10^{16} cm^{-2} was performed selectively to 36 μm wide regions on the Type II sample to form metal-gettering regions,[17–19] which locates equally from two neighboring MIC windows. The 50-nm thick Ni was then deposited by electron-beam evaporation and 10 h pre-annealing at 400 °C was performed for the outdiffusion of hydrogen from the a-Si:H layer. The MIC heat-treatment was then carried out in nitrogen atmosphere at 550 °C for 24 h for Type-I samples and 600 °C for 2.5 h for Type-II samples, respectively.

*Project supported by the National Natural Science Foundation of China (Grant Nos. 61301077 and 61574096), the Natural Science Foundation of Jiangsu Province, China (Grant No. BK20130319), and the Science and Technology Program of Suzhou City, China (Grant No. SYG201538).

†Corresponding author. E-mail: mingxiang_wang@suda.edu.cn

© 2017 Chinese Physical Society and IOP Publishing Ltd

The morphology of the sample surface after the MIC heat-treatment was studied under an optical microscope, which was also used to measure the dimensions of the MIC poly-Si region and the a-Si region remained between the MIC poly-Si regions. The crystallinity characteristic was analyzed based on Renishaw InVia micro-Raman spectroscopy measurement with a lateral spatial resolution smaller than 1 μm. Lateral nickel distribution in the MIC poly-Si and the a-Si was measured with a PHI7200 time-of-flight secondary ion mass spectrometer (TOF-SIMS).

3. Results and discussion

Figure 1 shows a picture of a Type-I sample after 24-h heat-treatment at 550 °C, which includes two MIC windows. The MIC poly-Si region can be easily distinguished from the uncrystallized a-Si region by the color difference under the microscope. The length of MIC poly-Si regions is thus measured to be ∼ 50 μm and the lateral crystallization rate is estimated to be 2.1 μm/h. As the distance between the two neighboring MIC windows is ∼ 350 μm, there is an approximately 250 μm wide a-Si region separating the neighboring MIC poly-Si regions.

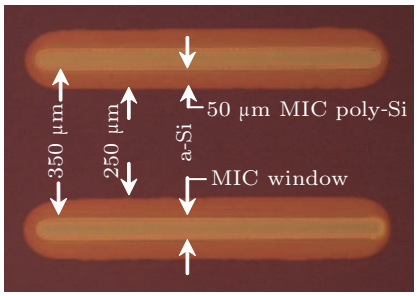


Fig. 1. (color online) Picture of a Type-I sample after MIC heat-treatment where the distance between the two neighboring MIC windows is 350 μm.

When the distance between the two neighboring MIC windows is reduced to about 250 μm, i.e., 150 μm wide a-Si region remains, a line-shaped region which shows similar but weaker color than the MIC poly-Si regions appears in the middle of the a-Si region as shown in Fig. 2(a). Furthermore, in the case when two neighboring MIC windows are separated by 160 μm as shown in Fig. 2(b), the line-shaped region becomes more obvious with an average width of 18 μm. Micro-Raman analysis was performed to the MIC poly-Si, the a-Si separating the MIC poly-Si regions, and the line-shaped region appeared in the a-Si, respectively. It can be seen from Fig. 3 that there is a signal peak locating at 480 cm^{-1} for the a-Si region, indicating that its amorphous nature remains. However, the characteristic amorphous peak is absent from the Raman spectra for the line-shaped region and the MIC poly-Si region, which confirms the crystalline nature of the line-shaped region appeared in the a-Si matrix.

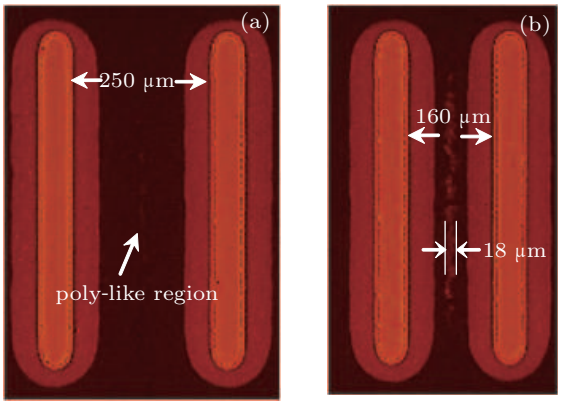


Fig. 2. (color online) Pictures for the morphology of the Type-I sample after the MIC heat-treatment. (a) The distance between the two MIC windows is 250 μm; (b) the distance between the two MIC windows is 160 μm.

The heat-treatment during the MIC process could lead to the crystallization of the a-Si due to the solid-phase crystallization (SPC) effect, but the SPC process usually needs a heat-treatment at a temperature higher than 600 °C and time of tens of hours, so the heat-treatment at 550 °C during the MIC process should not induce any crystallization effects. The heat accumulation could also enhance the crystallization and it is also dimension-related, but it is the crystallization front rather than the middle position of the a-Si region separating the crystallization fronts that is affected,[4] so there should be some different mechanism reasons for the observed crystallization phenomenon.

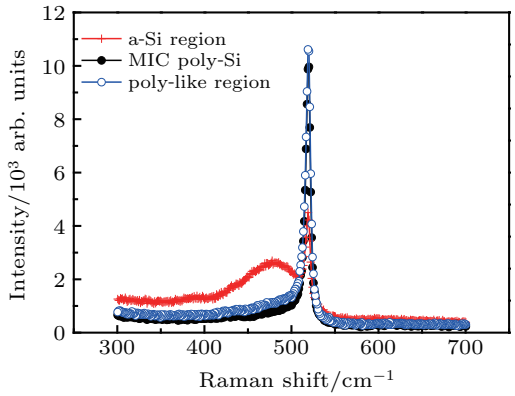


Fig. 3. (color online) Raman spectra for the a-Si region, MIC poly-Si region, and the poly-like region in the a-Si matrix.

Further careful observation of the morphology of the poly-Si appeared in the a-Si matrix shown in Fig. 2(b), which reveals that the crystallization edges are very ragged, which is similar to the typical morphology characteristic of MIC poly-Si region when the supply of nickel to the MIC front is insufficient.[14] It suggests that there could be some trace Ni distributed in the a-Si matrix in front of MIC poly-Si, which induces the crystallization of the a-Si when its local concentration is accumulated to be high enough.[11]

To verify the hypothesis that some trace Ni has diffused from the MIC windows into the a-Si matrix beyond the MIC

front during the MIC heat-treatment process, it would be convincing if nickel could be directly detected in the a-Si region. However, the nickel concentration in the a-Si region on the Type-I sample is too low to be detected by the TOF-SIMS, so Type-II samples with phosphorus-implanted metal-gettering regions are prepared. The gettering regions can collect those nickel atoms that have diffused into the a-Si all the way during the MIC process and increase the local nickel concentration to reach the detection limit of the TOF-SIMS. After the removal of the covering oxide, TOF-SIMS analysis is performed on the Type-II sample and the lateral distributions of nickel and phosphorus are plotted as shown in Fig. 4. As expected, it is observed that there is some trace nickel detected in the phosphorus implanted a-Si region. The relatively higher Ni concentration in the phosphorus-implanted a-Si region is believed to be the result of the collecting effect of the metal-gettering region on the nickel atoms that diffused into the a-Si beyond the MIC front.

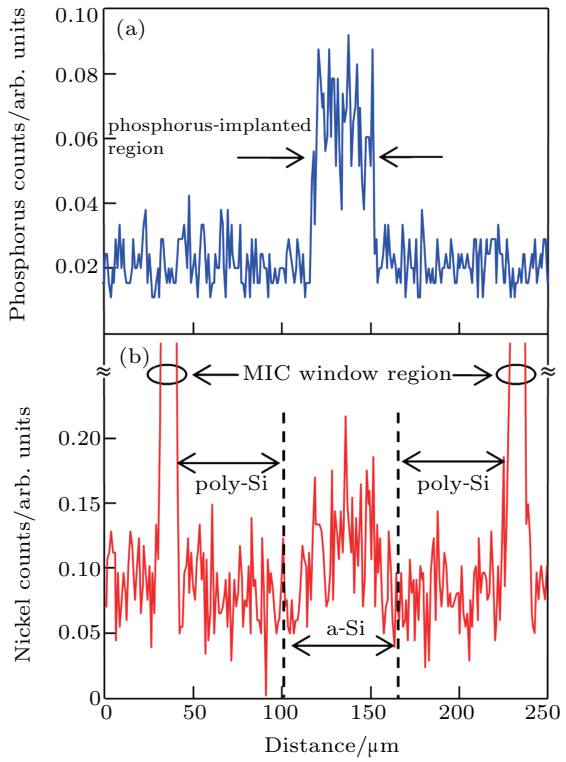


Fig. 4. (color online) Lateral distribution of (a) phosphorus and (b) nickel in the MIC poly-Si region and a-Si region on the Type-II sample.

The observed crystallization in the middle of the a-Si region between two MIC fronts can thus be explained as follows. During the MIC heat-treatment, each MIC window will contribute a nickel distribution in the a-Si, and the superposition of the two nickel distributions induced by the two neighboring MIC windows will provide a peak nickel concentration in the middle of the a-Si region between the two MIC windows. Local metal-induced crystallization occurs once the peak nickel concentration is high enough to form crystallization nuclei.[11] The shorter the distance between the two neighboring MIC windows is, the easier for the nickel to diffuse from the MIC windows to the middle of the a-Si matrix and accumulate there, resulting in a more observable line-shaped crystallized region as shown in Fig. 2.

The occurrence of the a-Si crystallization means that nickel has diffused from the MIC windows to the crystallization location during the MIC heat-treatment. Though there have been many investigations on metal diffusion in a-Si in the literature, reports on the diffusion of nickel in a-Si matrix are very limited.[20] One can notice from Fig. 2(a) that the crystallization takes place at the position of approximately 125 μm away from the MIC window, so the minimum diffusion length (L) of nickel at 550 °C in 24 h is 125 μm. Based on the diffusion length estimation equation $L = \sqrt{D_{\mathrm{Ni}}t}$, where D_{Ni} is the diffusion coefficient of Ni and t is the heat-treatment time, a minimum D_{Ni} in a-Si at 550 °C is estimated to be 1.84×10^{-9} cm^2/s, which is 56 times higher than the value of 3.28×10^{-11} cm^2/s that is extrapolated from lower temperature values.[20] With the previously reported diffusion coefficient of 3.28×10^{-11} cm^2/s, one could estimate a diffusion length much smaller than the MIC length and the distance between the MIC window and the observed line-shaped poly-Si region, so the reported D_{Ni} in this paper is more reliable for modeling the MIC process.

4. Conclusions

In this paper, the lateral diffusion and distribution of trace Ni in the a-Si matrix beyond the MIC poly-Si front during the MIC heat-treatment is discovered, which indicates that besides those Ni atoms formed silicide at the MIC front, some trace Ni atoms diffuse in the a-Si matrix beyond the MIC front at a rate much faster than the MIC rate. Such trace Ni could induce local crystallization of a-Si when its local concentration is accumulated to be high enough for crystallization nuclei formation. A minimum diffusion coefficient of 1.84×10^{-9} cm^2/s at 550 °C is thus estimated for trace Ni diffusion in a-Si based on the observation.

References

[1] Jang K, Lee W, Choi W and Yi J 2012 *Jpn. J. Appl. Phys.* **51** 09MF01
[2] Tankut A, Karaman M, Yildiz I, Canli S and Turan R 2015 *Phys. Status Solidi (a)* **212** 2702
[3] Li J, Wang J, Yin M, Gao P and He D 2006 *Chin. Phys. Lett.* **23** 3338
[4] Hsueh W C and Lee S C 2003 *IEEE Trans. Electron Devices* **50** 816
[5] Lee S W, Jeon Y C and Joo S K 1995 *Appl. Phys. Lett.* **66** 1671
[6] Lee S and Joo S 1996 *IEEE Electron Device Lett.* **17** 160
[7] Meng Z, Wang M and Wong M 2000 *IEEE Trans. Electron Devices* **47** 404
[8] Meng Z, Wu C, Li J, Xiong S, Kwok H S and Wong M 2005 *Acta Phys. Sin.* **54** 3363 (in Chinese)

[9] Choi J H, Cheon J H, Kim S K and Jang J 2005 *Displays* **26** 137

[10] Mizuki T, Matsuda J S, Nakamura Y, Takagi J and Yoshida T 2004 *IEEE Trans. Electron Devices* **51** 204

[11] Wu C Y, Li X D, Zhao S Y, Li J, Meng Z G, Xiong S Z and Zhang F 2009 *Chin. Phys. B* **18** 1237

[12] Li H, Li X, Li J, Wu C, Meng Z and Xiong S 2008 *Acta Phys. Sin.* **57** 2476 (in Chinese)

[13] Jin Z, Bhat G A, Yeung M, Kwok H S and Wong M 1998 *J. Appl. Phys.* **84** 194

[14] Yoon S Y, Park S J, Kim K H and Jang J 2001 *Thin Solid Films* **383** 34

[15] Miyasaka M, Makihira K, Asano T, Polychroniadis E and Stoemenos J 2002 *Appl. Phys. Lett.* **80** 944

[16] Ma T and Wong M 2002 *J. Appl. Phys.* **91** 1236

[17] Zhang D and Wong M 2005 *J. Soc. Inf. Display* **13** 815

[18] Wang B and Wu Y 2010 *J. Electron. Mater.* **39** 157

[19] Jiang L, Lu Z, Zhang F and Lu X 2013 *Acta Phys. Sin.* **62** 110101 (in Chinese)

[20] Kuznetsov A Y and Svensson B G 1995 *Appl. Phys. Lett.* **66** 2229